Research Article | Vol. 29, No. 8 / 12 April 2021 / Optics Express 11674
Optics EXPRESS

High power (>500W) cryogenically cooled Yb:YLF cw-oscillator operating at 995 nm and 1019 nm using E//c axis for lasing

MARTIN KELLERT,[1,*] UMIT DEMIRBAS,[1,2] JELTO THESINGA,[1] SIMON REUTER,[1] MIKHAIL PERGAMENT,[1] AND FRANZ X. KÄRTNER[1,3,4]

[1]Center for Free-Electron Laser Science, Deutsches Elektronen-Synchrotron DESY, Notkestraße 85, 22607 Hamburg, Germany
[2]Laser Technology Laboratory, Department of Electrical and Electronics Engineering, Antalya Bilim University, Antalya, Turkey
[3]Physics Department, University of Hamburg, Luruper Chaussee 149, 22761 Hamburg, Germany
[4]The Hamburg Centre for Ultrafast Imaging, Luruper Chaussee 149, 22761 Hamburg, Germany
*martin.kellert@cfel.de

Abstract: We present record continuous wave (cw) output power levels from cryogenically cooled Yb:$YLiF_4$ (Yb:YLF) lasers in rod geometry. The laser system is pumped by a state-of-the-art 960 nm diode module, and vertically polarized lasing was employed using the E//c axis of Yb:YLF. Lasing performance was investigated at different output coupling levels in different cavity configurations and the laser crystal temperature was estimated via monitoring the emission spectrum of the gain media. We have obtained a cw output power up to 400 W at a wavelength of 995 nm. The absorbed pump power was around 720 W, and the laser output had a TEM_{00} beam profile with an M^2 of 1.3 in both axes. At higher absorbed pump power levels with increasing laser crystal temperature, we observed a lasing wavelength shift from 995 nm to 1019 nm. In this regime cw output power levels above 500 W have been achieved at an absorbed pump power of 750 W. Further power scaling was limited by the onset of strong thermal lensing. We discuss underlying physical mechanisms for the wavelength shift and present detailed temperature measurements under lasing conditions.

1. Introduction

The advantage of Yb:YLF as laser gain material at cryogenic temperatures due to its relatively low quantum defect and good thermo-optic properties is well-known and widely studied for E//a and E//c axis [1,2,3,4]. Commercially available pump sources around 960 nm can be used to efficiently pump Yb:YLF crystals, which leads to a lower quantum defect in comparison to Yb:YAG, and, therefore, also to a lower crystal temperature. In the past, the main research interest was focused to the case of E//a operation, because of its broader gain bandwidth around 1016 nm and the potential for shorter pulses from regenerative amplifiers [5,6,7], multi-pass amplifiers [8,9], Q-switching schemes [10] and oscillators [11]. A maximum output power of >300 W [12] and output energies up to 305 mJ have been reported [9].

On the other hand, E//c operation shows a narrower gain profile at 995 nm with about two times higher gain cross section when compared to the 1019 nm transition [1,13]. In addition, the thermal conductivity along the c-axis is higher in comparison to the a-axis [14], which allows better heat extraction, and, therefore, lower peak temperature under the same pumping conditions. Also, the quantum defect when lasing at 995 nm is lower (3.5%), in comparison to the 1019 nm transition (5.7%) which leads to a lower heat load in the crystal [15]. This makes Yb:YLF in E//c axis a very attractive laser material for cw-lasing [13], cw-amplification [16] or

#422526 https://doi.org/10.1364/OE.422526
Journal © 2021 Received 15 Feb 2021; revised 23 Mar 2021; accepted 23 Mar 2021; published 30 Mar 2021

Optics EXPRESS

ns Q-switching [17]. Earlier results showed cw output power levels up to 224 W at 995 nm from a single, cryogenically cooled crystal [13], which was only limited by the available pump power. In addition, after almost one-decade, considerable improvements have been made in scaling of the output power from commercially available fiber coupled diodes at 960 nm. Furthermore, latest investigations [18] have found an even higher gain in E//c at the 995 nm emission peak in comparison to previous studies and an around 3-times higher gain cross section for the 1019 nm transition in comparison to E//a operations at the expense of reduced bandwidth. Combining all these advantages, it should be possible to further scale the output power of Yb:YLF rods to higher levels.

In this paper, we present lasing results using 1% doped Yb:YLF in E//c axis with different output couplers ranging from 25% to 70% for different cavity designs. We were able to reach ~400 W lasing at 995 nm and more than 500 W when lasing at 1019 nm which is, to the best of our knowledge, the highest output power from a single Yb:YLF rod at cryogenic temperatures. We observe a wavelength shift during lasing, leading to a two-color wavelength emission in the transition phase. We characterize output beam properties at different output power and present detailed temperature measurements under lasing conditions. We also discuss and present reasons for the observed wavelength shift.

2. Experimental setup

Figure 1(a) shows the basic cw laser cavity we use in our experiments. For pumping the 1% Yb:YLF gain media into the 960 nm absorption band [1], we use a commercially available 2 kW, temperature stabilized laser diode module (LDM) emitting un-polarized laser light at a center wavelength of 960 nm with 2.5 nm FWHM. The LDM with an estimated M^2 of around 220 is fiber coupled into a 600 µm, NA=0.22, fiber. The output from the fiber end is first collimated with a 72 mm focal length lens (f1) and then imaged via a second lens (f2) with focal length of 250 mm into the crystal. The pump beam image has a flat top beam profile with a spot diameter of around 2.1 mm. The crystal is a 1% Yb^{3+}-doped, 20 mm long crystal (15 mm width, 10 mm height) with two 3 mm thick undoped diffusion bonded end caps to reduce surface deformation under thermal load. The Yb:YLF crystal is used in E//c operation as shown in Fig. 1(b), and is one-sided cryogenically cooled with liquid nitrogen to 78 K. The gain element is soldered with indium to a metal heatsink perpendicular to the c-axis. The heatsink is then thermally contacted by compressing an indium gasket to the cooling plate of the Dewar to complete assembly; boiling liquid nitrogen in the dewar provides primarily cooling from the top. The crystal assembly is kept in a vacuum chamber at a pressure less than 10^{-6} mbar.

The short laser cavity consists of a flat dichroic mirror (DM), with a transmission for 960 nm of around 99%, a high reflectivity of 99.9% for 995 nm and a flat output coupler (OC). Note that, the measured reflectivity of the OC for the 960 nm pump light is in the same range as the reflectivity for 995 nm, which leads to additional heating of the dewar and crystal assembly due to back reflection of the unabsorbed pump power. The total length of the cavity is around 30 cm which is limited by the dimensions of the dewar. After collecting all short-cavity data the cavity is extended to around 150 cm and the flat dichroic mirror is exchanged by a curved DM with a radius of curvature of 15 m. The mode of the resulting semi-hemispherical cavity matches the pump beam size in the gain element and the designed cavity is also less sensitive to thermal lensing compared to a standard flat-flat cavity [19]. A pump separator with a transmission of 95% for 960 nm and a reflectivity of 99,9% for 995 nm is introduced to avoid back reflection of unabsorbed pump light into the Dewar, hence reducing additionally thermal loading. Two additional thin film polarizers (TFP) are installed to define the intra-cavity polarization and also in preparation for further Q-switching and cavity dumping experiments.

Optics EXPRESS

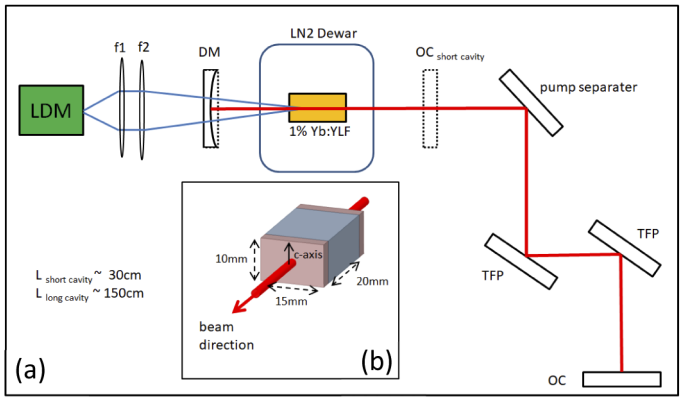

Fig. 1. (a) Experimental setup of cryogenic cooled cw-amplifier pumped by a 2 kW, 960 nm laser diode module (LDM), dotted mirrors shows short cavity with flat dichroic mirror (DM) and flat output coupler (OC); long cavity with curved dichroic mirror (DM), pump separator to minimize reflected pump light into Dewar and flat output coupler (OC), thin-film-polarizer (TFP) to maintain intra-cavity polarization and as preparation for further experimentation, (b) 1% Yb:YLF gain medium, axis orientation and dimensions.

3. Experimental results

3.1. Short cavity continuous wave lasing results

We start by presenting the cw lasing results for the short cavity. Figure 2(a) shows the measured cw laser performance of the cryogenic Yb:YLF laser using different output couplers with transmission in the 25-70% range. During the experiments, at low pump power levels the system starts to lase at 995 nm, which then jumps to 1019 nm at elevated temperatures (shown by empty markers). Note that, the wavelength shift is sometimes accompanied by a discontinuity in the slope of the graphs due to a changing quantum defect. As an example, for the 25% OC we observe a jump in lasing wavelength at a laser output power of around 30 W. By increasing the OC, we are able to stretch the switching point to 183 W at 40%, 294 W at 60% and 361 W at 70%. In the transition phase from 995 nm to 1019 nm we observe two-color lasing operation. Above this point we see only lasing at a wavelength of 1019 nm and the slope has a lateral shift, however the slope is unchanged. We will discuss the effect of wavelength switching in more detail in section 4. Increasing the pump power further leads, to the best of our knowledge, to the highest extracted power of 514 W from any Yb:YLF system to date. Note that, the calculated slope efficiency of the laser for each output coupling is also shown in Fig. 2 (a) as an inset. The efficiency numbers in Fig. 2(a) is fitted over the whole curve, except for 70% OC were we not consider the parallel shift when the wavelength shift occurred, which would lead to a slightly lower slope efficiency. Figure 2(b) shows, as an example, the near field beam profile at selected output power levels for 60% output coupling. At low power up to 30 W, the beam is close to a Gaussian TEM_{00} mode, above 30 W the laser beam changed to a flattened Gaussian beam [20]. Beyond 450 W the beam profile is turning more and more to a TEM_{30} mode, because higher-order transverse modes become more dominant [21]. The estimated pump absorption is around 95% at highest pump power. The pump diode module is not wavelength stabilized and the diode temperature is optimized to exactly match the 960 nm absorption peak at highest output power level.

Figures 3(a) and (b) show examples of output spectra at selected output power levels for output coupling of 25% and 60%, respectively. For spectral measurements we use a custom-modified Ocean Optics HR4000 spectrometer with a spectral resolution of 0,1 nm in the range of 900-1060 nm. As discussed earlier, we have seen lasing at 995 nm at low pump power, and a transition

Optics EXPRESS

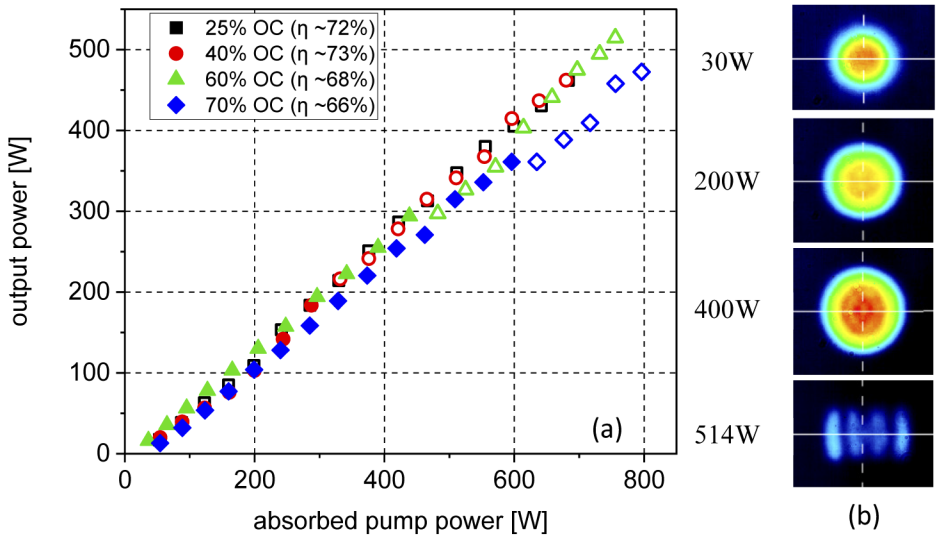

Fig. 2. (a) Short cavity cw lasing results, output power with different output couplers (OC) 25%, 40%, 60% and 70%, filled markers representing 995 nm lasing, empty markers 1019 nm lasing, (b) Near field beam profile at selected output power levels for 60% OC.

to 1019 nm band as the pump power is increased. At low output coupling of 25% the wavelength tends to switch already at around 30 W and we observe two-color lasing. Above this power level the wavelength stays at 1019 nm. The same behavior is observed with 60% output coupling, where the switching point is around 300 W. Here, it is clearly seen that in the transition range the wavelength shift does not happen instantaneously but rather continuously. The intensity of the 1019 nm line is rising slowly whereas the 995 nm peak is reduced. The laser spectra have a width (FWHM) of around 0.15 nm for 995 nm lasing and 0.3 nm for 1019 nm lasing. We believe the 995 nm lasing width is narrower compared to 1019 nm lasing due to the sharper gain cross section of the 995 nm transition. Again, we will discuss this behavior in more detail in section 4.

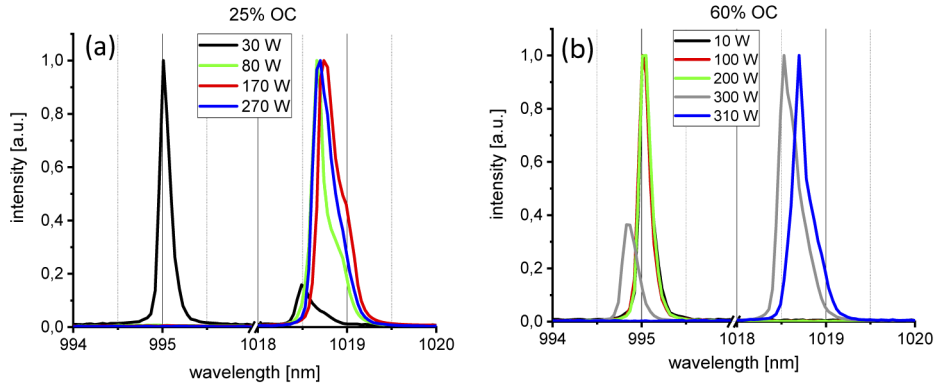

Fig. 3. Sample spectra of the cw Yb:YLF laser at different output power levels for (a) 25% and (b) 60% output coupling, respectively.

Optics EXPRESS

3.2. Long cavity continuous wave lasing results

For the long cavity configuration, as mentioned in section 2, the cavity is extended to a total length of 150 cm and the flat dichroic mirror is exchanged by a curved dichroic mirror with a radius of curvature of 15 m. We start this subsection with Fig. 4, which shows the measured cw laser performance of the cryogenic Yb:YLF laser for the long standing-wave cavity configuration. The slope efficiency of the long cavity laser is slightly lower for all output couplers when compared to the short cavity. The lasing threshold is raised due to increased cavity losses caused by additional optical elements. We estimate the additional losses due to insertions of TFP´s and pump separator to around 3%. The output laser beam has a TEM_{00} profile at all power levels compared to the almost flat-top or strongly multimode beam profile at higher power levels for the short cavity. Hence, the mode matching between pump and intracavity laser mode is better for the case of a short cavity, at the expense of reduced beam quality.

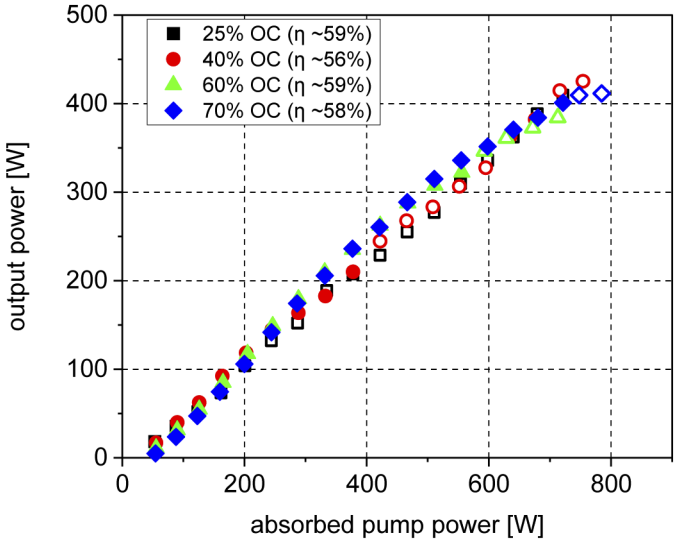

Fig. 4. long cavity lasing results, output power with different output couplers (OC) 25%, 40%, 60% and 70%, filled markers representing 995 nm lasing, empty markers 1019 nm lasing

The pump absorption is comparable to our short cavity and is estimated to be around 95% at highest pump power. Compared to our short cavity results we were able to shift the wavelength switching point from 995 nm to 1019 nm further to 35 W at 25%, 210 W at 40%, 322 W at 60% and 402 W at 70% OC. This is due to the reduced thermal load introduced by the back reflection of unabsorbed pump of the outcoupling mirror in our short cavity. The reflectivity of the OC for 960 nm pump light is in the range of its output coupling grade for 995 nm. Using a pump separator minimizes back reflection, hence reducing the thermal load of the crystal. Here we get a first hint, that peak temperature is influencing the lasing wavelength of the laser. To underline this statement, we will present detailed temperature estimations in the following section.

To complete our experimental results, we measure the M^2 using 70% output coupling, where we reached the highest output power at 995 nm. Figure 5 (a)-(d) shows detailed measurements of M^2 at different output power using a f = 300 mm lens. We estimate the M^2 at 400 W to around 1.3, but we would like to mention that starting from 300 W we observe a deformation of the beam around the foci. As mentioned in the experimental setup, our crystal is only cooled from one side to cryogenic temperatures. Simulations in [22] shows, that one-sided cooling of a bonded Yb:YLF crystal, similar to the one we use in this study, introduces an asymmetric thermal lens

Optics EXPRESS

on the front and back surface. This asymmetry causes asymmetric spherical aberration and is transferred into the far field.

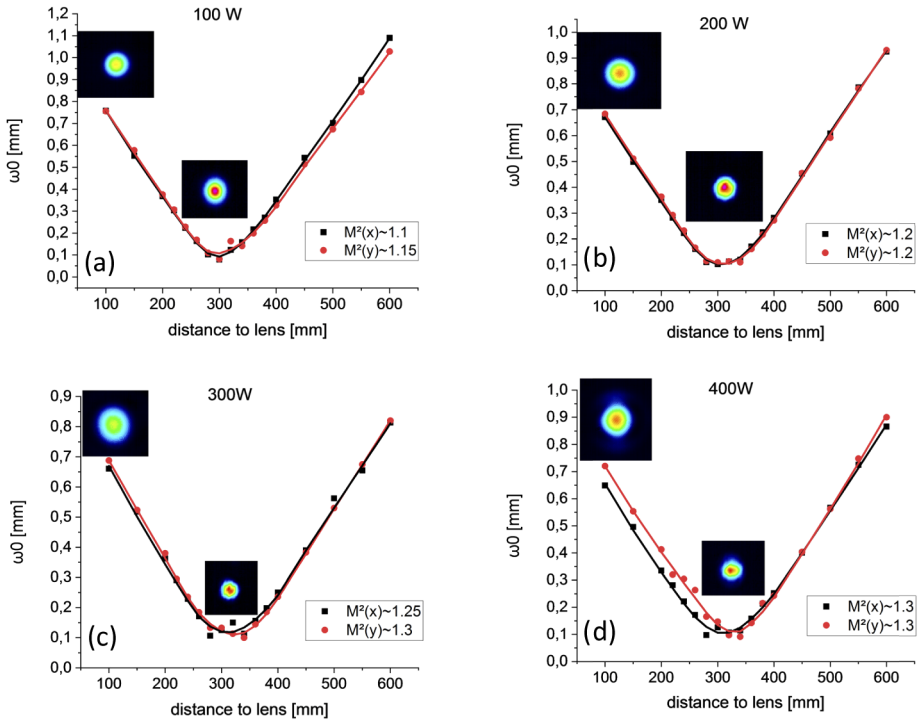

Fig. 5. (a)-(d) Measured caustic at 70% output coupling using a 300 mm focal length lens at (a) 100 W, (b) 200 W, (c) 300 W, and (d) 400 W output power levels for 995 nm lasing. Inset pictures show beam profiles at near and far-field.

We summarize the results of the short and long cavity experiments in Table 1, where we highlight the maximum output power reached.

Table 1. Overview of maximum output power at 995 nm and 1019 nm using different output couplers.

Output coupling [%]	Maximum output power [W] at λ = 995 nm		Maximum output power [W] at λ = 1019 nm	
	Short cavity	Long cavity	Short cavity	Long cavity
25	30	35	462	410
40	183	210	462	425
60	294	322	**514**	384
70	361	**402**	472	411

4. Temperature estimation under lasing conditions and discussion of observed wavelength shift

It was already demonstrated in [23], that uniaxial Nd:YLF has the property to generate laser emission at different wavelength simultaneously when optimizing the peak temperature in the gain media. A temperature dependent wavelength competition in Er:YAG was also shown in [24], where a laser wavelength of 1618 nm below 90 K and 1645 nm above 110 K was observed.

Optics EXPRESS

To understand the observed behavior of lasing at different wavelengths for different output couplers and peak temperatures in our study, one needs to go back to spectroscopic properties of Yb:YLF in E//c axis under cryogenic temperatures. These properties have been investigated in great detail [18], and here we will concentrate on the gain cross section (GCS) under different temperature conditions and inversion levels. In our analysis, we will focus only on GCS at 995 nm and 1019 nm and compare their relation under different conditions. The gain cross section spectra are estimated using

$$\sigma_g(\lambda, T) = \beta\sigma_e(\lambda, T) - (1 - \beta)\sigma_a(\lambda, T) \quad (1)$$

where β is the fractional population inversion level, σ_e the emission cross section and σ_a the absorption cross section.

In Fig. 6, we show the calculated variation of GCS of Yb:YLF for E//c. Figure 6 (a) shows the GCS spectra at a crystal temperature of 125 K for different inversion levels between 0.05 and 0.25. Whereas in Fig. 5 (b), we show the variation of GCS with temperature at a fixed inversion level of 0.15. As we can see from Fig. 5(a), as expected the GCS value of Yb:YLF is decreasing with decreasing inversion level due to increasing self-absorption losses. Also, as the inversion decreases, the GCS for 995 nm, which is dominant in E//c axis for high inversion levels, is first becoming equal and finally becoming weaker than GCS of 1019 nm due to the increased role of self-absorption losses at shorter wavelengths. At 125 K and inversion of around 10% the GCS for 1019 nm is higher than 995 nm, hence lasing at 1019 nm is preferred. From this, we can conclude that at high inversion levels 995 nm lasing is favored. This property explains our observed behavior that, with increasing output coupling, we can shift the switching point from 995 nm to 1019 nm to higher output power levels. Furthermore, as shown in Fig. 5(b) the same behavior of GCS is true for fixed inversion and different temperatures in the gain media. For an inversion level of 15% the GCS of 995 nm and 1019 nm transition becomes equal for laser crystal temperatures in the 125-150 K range. At a fixed inversion level, 995 nm lasing is preferred at lower crystal temperatures.

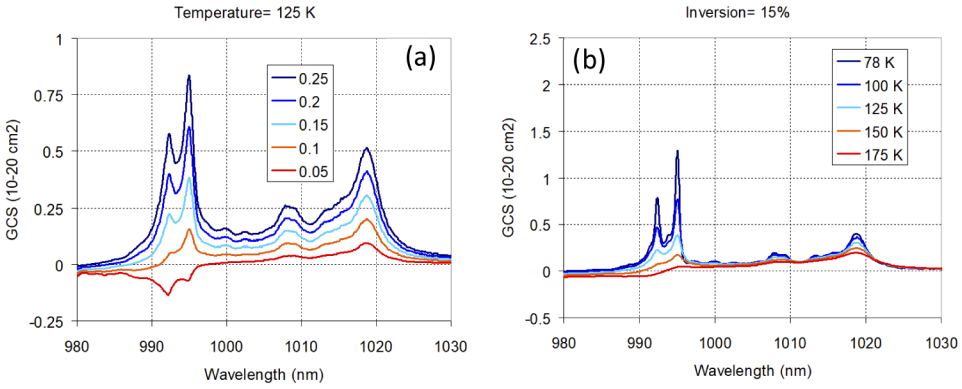

Fig. 6. Reference [18] wavelength depended gain cross section (GCS) for 1% doped Yb:YLF, E//c axis at, (a) at a fixed temperature of 125 K and inversion levels between 5 and 25%, (b) at a fixed inversion level of 15% at different temperatures between 78 and 175K

To underline our statements, we present detailed temperature estimates under lasing conditions, taken during the experiments described in section 3. We use a modified temperature probing technique presented in [25], where we use the change in the emission spectra to estimate the average temperature in the gain media. As shown in Fig. 7(a) the switching point to 1019 nm lasing is shifting to higher absorbed power with higher output coupling (higher inversion), independent from the peak temperature in the crystal. We also observe a sudden jump to higher

Optics EXPRESS

temperature when the lasing wavelength shifts, especially at OC grades of 60% and 70%. This is due to the change in quantum defect which is defined by

$$q = h\nu_{pump} * \left(1 - \frac{\lambda_{pump}}{\lambda_{laser}}\right) \tag{2}$$

where, when switching from 995 nm to 1019 nm, the wavelength difference between pump and laser is rapidly increasing.

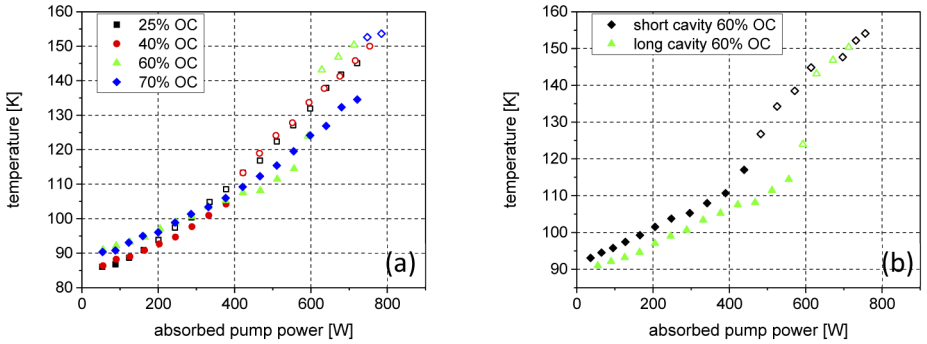

Fig. 7. (a) Temperature estimation in 1% doped Yb:YLF crystal under lasing conditions for the long cavity laser, at different pump absorption with different output couplers 25%, 40%, 60% and 70%, (b) temperature estimation under lasing conditions at different pump absorption for long and short cavity at 60% OC, filled markers representing 995 nm lasing, empty markers 1019 nm lasing.

The same observation is true for the temperature measurements shown in Fig. 7(b), taken at the same output coupling value but different cavity configurations. The reader is reminded that we used output couplers with almost the same reflectivity for 995 nm and 960 nm wavelength. In the short cavity the unabsorbed pump light is reflected back into the dewar and crystal assembly, leading to an additional heating of the gain media. Here we clearly see that, at the same inversion level the switching point to 1019 nm is shifted to higher absorbed power in the long cavity due to the lower average temperature in the crystal as a consequence of reduced pump back reflection. As a side note, above temperatures of 150 K the laser becomes unstable and very difficult to align for all output coupling values used. Due to the onset of an asymmetrical thermal lens the laser mode tends to drift away from its optimum alignment which leads to lower extraction hence more stored heat inside the crystal. This leads to an interplay between extraction and peak temperature which is difficult to balance.

5. Conclusion

We presented, to the best of our knowledge, the highest obtained average power from a single Yb:YLF rod of 402 W at 995 nm and 514 W at 1019 nm lasing wavelength. We characterized output beam properties at different output power and presented detailed temperature measurements under lasing conditions. We also discussed and gave reasons for the observed wavelength shifts. These results we will be able to scale the output power of regenerative amplifiers [12] and multi pass amplifiers [9] at 1019 nm further and open the path of a new generation of regenerative and multi pass amplifiers at 995 nm and 1019 nm.

Funding. Seventh Framework Programme (FP7/2007- 2013); European Research Council (609920).

Acknowledgments. The authors acknowledge support from previous group members L. E. Zapata, K. Zapata for establishing the indium-bonding technology for YLF at CFEL-DESY. UD acknowledges support from BAGEP Award of the Bilim Akademisi.

Optics EXPRESS

Disclosures. The authors declare no conflicts of interest.

References

1. T. Y. Fan, D. J. Ripin, R. L. Aggarwal, J. R. Ochoa, B. Chann, T. Tilleman, and J. Spitzberg, "Cryogenic Yb^{3+}-Doped Solid-State Lasers," IEEE J. Sel. Top. Quantum Electron. **13**(3), 448–459 (2007).
2. J. Kawanaka, S. Tokita, H. Nishioka, M. Fujita, K. Yamakawa, K. Ueda, and Y. Izawa, "Dramatically improved laser characteristics of diode-pumped Yb-doped materials at low temperature," Laser Phys. **15**, 1306–1312 (2005).
3. A. Bensalah, Y. Guyot, A. Brenier, H. Sato, T. Fukuda, and G. Boulon, "Spectroscopic properties of Yb^{3+}: LuLiF4 crystal grown by the Czochralski method for laser applications and evaluation of quenching processes: a comparison with Yb^{3+}: YLiF4," J. Alloys Compd. **380**(1-2), 15–26 (2004).
4. A. Bensalah, Y. Guyot, M. Ito, A. Brenier, H. Sato, T. Fukuda, and G. Boulon, "Growth of Yb^{3+}-doped YLiF4 laser crystal by the Czochralski method. Attempt of Yb^{3+} energy level assignment and estimation of the laser potentiality," Opt. Mater. **26**(4), 375–383 (2004).
5. H. Cankaya, U. Demirbas, Y. Hua, M. Hemmer, L. E. Zapata, M. Pergament, and F. X. Kärtner, "190-mJ Cryogenically-Cooled Yb:YLF Amplifier System at 1019.7 nm," OSA continuum (2019).
6. J. Kawanaka, K. Yamakawa, H. Nishioka, and K.-I. Ueda, "30-mJ, diode-pumped, chirped-pulse Yb:YLF regenerative amplifier," Opt. Lett. **28**(21), 2121–2123 (2003).
7. U. Demirbas, H. Cankaya, Y. Hua, J. Thesinga, M. Pergament, and F. X. Kärtner, "20-mJ, sub-ps pulses at up to 70 W average power from a cryogenic Yb:YLF regenerative amplifier " Opt," Opt. Express **28**(2), 2466–2479 (2020).
8. D. E. Miller, L. E. Zapata, D. J. Ripin, and T. Y. Fan, "Sub-picosecond pulses at 100 W average power from a Yb:YLF chirped-pulse amplification system," Opt. Lett. **37**(13), 2700–2702 (2012).
9. Y. Liu, U. Demirbas, M. Kellert, J. Thesinga, H. Cankaya, Y. Hua, L. E. Zapata, M. Pergament, and F. X. Kärtner, "Eight-pass Yb:YLF cryogenic amplifier generating 305-mJ pulses," OSA Continuum **3**(10), 2722–2729 (2020).
10. D. E. Miller, J. R. Ochoa, and T. Y. Fan, "Cryogenically cooled, 149 W, Q-switched, Yb:LiYF4 laser," Opt. Lett. **38**(20), 4260–4261 (2013).
11. U. Demirbas, J. Thesinga, H. Cankaya, M. Kellert, F. X. Kärtner, and M. Pergament, "High-power passively mode-locked cryogenic Yb:YLF laser," Opt. Lett. **45**(7), 2050–2053 (2020).
12. U. Demirbas, H. Cankaya, J. Thesinga, F. X. Kärtner, and M. Pergament, "Efficient, diode-pumped, high-power (>300W) cryogenic Yb:YLF laser with broad-tunability (995-1020.5 nm): investigation of E//a-axis for lasing," Opt. Express **27**(25), 36562–36579 (2019).
13. L. E. Zapata, D. J. Ripin, and T. Y. Fan, "Power scaling of cryogenic Yb:LiYF4 lasers," Opt. Lett. **35**(11), 1854–1856 (2010).
14. R. L. Aggarwal, D. J. Ripin, J. R. Ochoa, and T. Y. Fan, "Measurement of thermo-optic properties of Y3Al5O12, Lu3Al5O12, YAIO(3), LiYF4, LiLuF4, BaY2F8, KGd(WO4)(2), and KY(WO4)(2) laser crystals in the 80-300 K temperature range," J. Appl. Phys., 98 (2005).
15. V. Ashoori, M. Shayganmanesh, and S. Radmard, "Heat Generation and Removal in Solid State Lasers," in *An Overview of Heat Transfer Phenomena*, S. N. Kazi, ed. (IntechOpen, 2012).
16. J. Manni, D. Haris, and T. Y. Fan, "High gain (43 dB), high power (40W), highly efficient, multipass amplifier at 995 nm in Yb:LiYF4," Opt. Commun. **417**, 54–56 (2018).
17. N. Ter-Gabrielyan, V. Fromzel, T. Sanamyan, and M. Dubinskii, "Highly-efficient Q-switched Yb:YLF laser at 995 nm with a second harmonic conversion," Opt. Mater. Express **7**(7), 2396–2403 (2017).
18. U. Demirbas, J. Thesinga, M. Kellert, F. X. Kärtner, and M. Pergament, "Detailed investigation of absorption, emission and gain in Yb:YLF in the 78-300 K range," Opt. Mater. Express **11**(2), 250–272 (2021).
19. W. Koechner, "Solid-State Laser Engineering," 6th edition, Springer-Verlag, chapter 5.
20. V. Bagini, R. Borghi, F. Gori, A. M. Pacileo, M. Santarsiero, D. Ambrosini, and G. S. Spagnolo, "Propagation of axially symmetric flattened Gaussian beams," J. Opt. Soc. Am. **13**(7), 1385–1394 (1996).
21. N. Hodgdon and H. Weber, "Laser Resonators and Beam Propagation," 2nd edition, Springer Verlag, chapter 5
22. U. Demirbas, H. Cankaya, J. Thesinga, F. X. Kärtner, and M. Pergament, "Power and energy scaling of rod-type cryogenic Yb:YLF regenerative amplifiers," J. Opt. Soc. Am. B **37**(6), 1865–1877 (2020).
23. C. Y. Cha, T. L. Huang, S. M. Wen, Y. J. Huang, K. F. Huang, and Y. F. Chen, "Nd:YLF laser at cryogenic temperature with orthogonally polarized simultaneous emission at 1047 nm and 1053 nm," Opt. Express **22**(21), 25318 (2014).
24. N. Ter-Gabrielyan, M. Dubinskii, G. A. Newburgh, A. Michael, and L. D. Merkle, "Temperature Dependence of a Diode-Pumped Cryogenic Er:YAG Laser," Opt. Express **17**(9), 7159–7169 (2009).
25. U. Demirbas, J. Thesinga, M. Kellert, F. X. Kärtner, and M. Pergament, "Comparison of different in situ optical temperature probing techniques for cryogenic Yb:YLF," Opt. Mater. Express **10**(12), 3403–3413 (2020).